Food Hydrocolloids 143 (2023) 108885

Contents lists available at ScienceDirect

Food Hydrocolloids

journal homepage: www.elsevier.com/locate/foodhyd

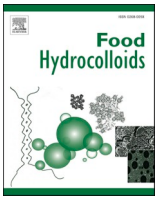

# Physical, interfacial and foaming properties of different mung bean protein fractions

Jack Yang [a,*,1], Qiuhuizi Yang [a,1], Babet Waterink [a], Paul Venema [a], Renko de Vries [b], Leonard M.C. Sagis [a]

[a] Laboratory of Physics and Physical Chemistry of Foods, Wageningen University, Bornse Weilanden 9, 6708WG, Wageningen, the Netherlands
[b] Laboratory of Physical Chemistry and Soft Matter, Wageningen University, Stippeneng 4, 6708 WE, Wageningen, the Netherlands

ARTICLE INFO

*Keywords:*
Mung bean protein
Dry fractionation
Protein coacervates
Protein fractionation
Interfacial rheology
Foams

ABSTRACT

Mung bean is an upcoming source of plant proteins with good foaming properties. The relation between its foaming properties and interfacial properties has not received much attention and was addressed in this work. To this end, five different mung bean protein fractions were produced. First, a protein-rich flour was obtained using dry fractionation, which was further processed into a protein mixture using mild wet fractionation to remove starch granules and other insoluble components. The protein mixture was further treated by isoelectric point precipitation to obtain a globulin- and albumin-rich fraction. Finally, we used the protein nativity of the dry fractionated flour to create protein coacervate droplets via liquid-liquid phase separation of the proteins at slightly acidic pH. The protein-rich coacervate droplets were heated and cross-linked into gelled particles, or "protein colloids". The interfacial and foam-stabilising properties of the flour and protein mixture were dominated by the globulins, producing a foam with a poor stability. Also, non-proteinaceous components, such as starch granules, phenols and phospholipids, seemed to reduce foam stability. Albumins formed substantially stiffer interfaces, leading to foams with a high stability. The highest foam stability was observed for the protein colloids, which we attribute to the formation of stiff interfacial layers and probably also pinning of the lamellae in the foams by the protein colloids. In summary, mung bean albumins were found to possess substantially better foaming properties than the globulins, but especially mung bean protein colloids are a promising candidate for a plant-based foam ingredient.

## 1. Introduction

The interest in plant-based alternatives for animal-based ingredients is rapidly growing. One of these animal-based ingredients to be replaced is egg white, which acts as a widely used foaming agent in a variety of aerated food products, such as meringue, cake and mousse. An upcoming and promising plant-based alternative for egg white is mung bean (MB) (Brishti et al., 2017; Du et al., 2018; Yi-Shen, Shuai, & Fitzgerald, 2018). It is a widely cultivated legume crop in Asia, Southern Europe, and Northern America. MB is high in essential amino acids and bioactive proteins/peptides (Kudre, Benjakul, & Kishimura, 2013; Yi-Shen et al., 2018). The major component in the seeds are carbohydrates, mostly present as starch granules, which can comprise between 55 and 65% (w/w) of the seed. The second largest fraction are proteins, which are responsible for 20–33% (w/w) of the seed. Also, MB contains about 1–1.85% (w/w) fat, which is favourable for protein fractionation, as defatting is not required (Anwar, Latif, Przybylski, Sultana, & Ashraf, 2007; Brishti et al., 2017; Ganesan & Xu, 2018; Mubarak, 2005). MB proteins have been studied for their foaming properties, but an extensive characterisation of their interfacial properties is lacking (Brishti et al., 2017; Du et al., 2018). Therefore, here we aim to perform a detailed study to fully understand the interface and foaming properties of MB proteins, fractionated and processed in various ways.

Plant proteins are commonly used as foaming ingredients. Conventional fractionation involves extensive wet processing. Seeds are milled and dispersed at alkaline pH for optimal protein solubility and yield. (Barać, Pešić, Stanojević, Kostić, & Čabrilo, 2015; Du et al., 2018; Kudre et al., 2013; H. Liu, Liu, Yan, Cheng, & Kang, 2015; Tang & Sun, 2010). Next, non-soluble components, such as starch granules and cell wall material, are removed by centrifugation or filtration. The resulting

* Corresponding author.
*E-mail address:* jack.yang@wur.nl (J. Yang).
[1] Co-first author.

https://doi.org/10.1016/j.foodhyd.2023.108885
Received 1 February 2023; Received in revised form 10 May 2023; Accepted 16 May 2023
Available online 29 May 2023

supernatant is high in protein content, but also in other solutes, such as sugars, salts, and phenols. These solutes can be removed by precipitating the proteins at their isoelectric point (pI), which is generally performed between pH 4–5 for MB protein (Brishti et al., 2017; Du et al., 2018; Kudre et al., 2013). Finally, the precipitated proteins are obtained and further processed into a protein isolate.

This above-mentioned wet fractionation method has several disadvantages, as it involves many processing steps, each requiring copious amounts of energy and water (Lie-Piang, Braconi, Boom, & van der Padt, 2021). Another drawback is a side stream after the second centrifugation step (after iso-electric precipitation) (Chua & Liu, 2019). The major protein fraction in legumes are the storage protein globulins and albumins (Chéreau et al., 2016; Lam, Can Karaca, Tyler, & Nickerson, 2018), with globulins being defined as being soluble in dilute-saline solutions, and albumins being defined as being soluble in pure water (Osborne, 1924). The globulins often have a pI between pH 4 and 5, while albumins are typically soluble in a wide pH range from 2 to 12 (González-Pérez, Vereijken, van Koningsveld, Gruppen, & Voragen, 2005). This suggests that the precipitate after isoelectric point precipitation mainly contains globulins, while the supernatant mainly contains the albumins. Yi-Shen et al. reported that 60% (w/w) of the protein in the MB seeds comprises of globulins, while 25% (w/w) of the proteins are albumins (Yi-Shen et al., 2018). As a result, up to 25% (w/w) of the MB proteins might be lost after the pI precipitation step. Extensive processing leads to higher proteins purity, but higher purities are often correlated to lower protein yields (Loveday, 2020; Tamayo Tenorio, Kyriakopoulou, Suarez-Garcia, van den Berg, & van der Goot, 2018). Avoiding the precipitation step, thus using a milder fractionation process, would significantly increase the protein yield (Tamayo Tenorio et al., 2018). Another major advantage of a milder fractionation process that avoids iso-electric precipitation is that changes in protein structure may be avoided. Such changes do occur with pI precipitation, and are linked to the aggregation of globulins, and to lower protein solubility (Geerts, Nikiforidis, van der Goot, & van der Padt, 2017; Pelgrom, Boom, & Schutyser, 2014).

The most energy-consuming step in wet fractionation is the final drying step, which is often performed by freeze-drying in scientific studies, or spray-drying or drum-drying on industrial scales. Avoiding the drying step would significantly increase the sustainability aspect of plant-based protein ingredients (Lie-Piang et al., 2021). An alternative purification method that avoids drying is dry fractionation. Proteins in seeds are stored in so-called protein bodies with typical sizes between 1 and 3 μm (Pernollet, 1978), whereas starch granules have larger sizes in the ranging of 7–26 μm for MB (Hoover, Li, Hynes, & Senanayake, 1997). By carefully milling MB seeds, protein bodies and starch granules can be detached from each other. Since protein bodies and starch granules differ in size and weight, the two fractions can subsequently be separated by air classification. The result is a flour separated into a coarse fraction rich in starch granules, and a fine fraction (FF) rich in protein bodies. The MB FF is a first MB protein fraction, which we will study for its interfacial and foaming behaviour. Next to reducing water and energy usage, dry fractionation fully preserves the native structure of the protein resulting in higher functionality, for example in foaming. Some starch granules may still be present in the fine fraction, and these may affect the foaming properties of MB proteins purified in this way. Therefore, we also use a combination of dry fractionation and wet-processing step to furthermore remove the starch granules (Zhang et al., 2015). This mildly purified protein mixture (PM) is a second sample we will use to study MB protein foaming. Of course, a drawback of using FF and PM, which have low protein contents, is the presence of non-proteinaceous components (e.g. starch, sugars and minerals). A third and fourth sample are more extensively purified globulin-rich (GLOB) and the albumin-rich (ALB) fractions, obtained from the PM fraction.

Finally, we also study heat-processed MB proteins for their foaming properties. We use a process to aggregate MB proteins recently described by some of us, resulting in MB protein aggregates previously called MB "protein colloids" (Q. Yang, Venema, van der Linden, & de Vries, 2023). Colloidal particles and protein aggregates are known to enhance the stability of protein-stabilised foams by increasing the viscosity of the liquid phase or by blocking the lamellae and/or plateau borders of the foam. Both phenomena can result in slower drainage of the foam, leading to more stable foams (Dhayal, Delahaije, de Vries, Gruppen, & Wierenga, 2015; Rullier, Novales, & Axelos, 2008, 2009). The protein colloids are produced from the PM fraction by adjusting the pH to slightly acidic pH values, leading to the formation of protein-rich, submicron droplets (protein coacervates) in a continuous protein-poor phase. These protein droplets are subsequently gelled by a heating step. This is a relatively simple method to create protein colloids. Protein colloids produced in this way can be regarded as nanogels or microgels, and could also be used for other functions, such as fat replacement, encapsulation and targeted delivery in the food industry (Inthavong, Chassenieux, & Nicolai, 2019; Karaca, Güven, Yasar, Kaya, & Kahyaoglu, 2009; Sağlam et al., 2013; Sandoval-Castilla, Lobato-Calleros, Aguirre-Mandujano, & Vernon-Carter, 2004; Shewan & Stokes, 2013). This is the last sample (COL) for which we will study MB protein interfacial and foaming properties.

In summary, the interfacial and foam-stabilising properties of five different MB protein fractions were studied, which is a novel element of this work, as this includes mung bean protein fractions with increasing protein purity:

1. a dry-fractionated fine fraction (FF).
2. a mildly purified protein fraction (PM).
3. a globulin-rich fraction (GLOB).
4. an albumin-rich fraction (ALB).
5. the protein colloids (COL).

For these fractions, a detailed physicochemical characterisation was performed, and interfacial properties were evaluated using large amplitude oscillatory dilatation (LAOD) in drop tensiometry. Foam stability for foams obtained from the different MB fractions was studied using whipping and sparging methods. While foaming of mung bean proteins has received attention in recent studies (Hadidi, Jafarzadeh, & Ibarz, 2021; Herneke, Karkehabadi, Lu, Lendel, & Langton, 2023; F. F. Liu et al., 2022; Shrestha, van't Hag, Haritos, & Dhital, 2023), little is still known about the interfacial properties. Our comprehensive approach especially aims at establishing a relation between the nature of the different MB protein fractions and their ability to act as a foaming agent.

## 2. Experimental section

### 2.1. Materials

Dried mung bean seeds (GC Mung Bean, Thailand) were obtained from online Asian store MyEUshop (The Netherlands). All chemicals (Sigma-Aldrich, USA) and materials for SDS-PAGE (Invitrogen Nove, Thermo Fisher Scientific, USA) were used as received. The samples were prepared in water (MilliQ Purelab Ultra, Darmstadt, Germany), unless stated differently.

### 2.2. Sample preparation

#### 2.2.1. Preparation of dry fractionation fine fraction

Mung beans (MB) were dry fractionated at a batch size of 400 g using a Multimill Hosakawa System (Hosakawa, Germany) equipped with a ZPS50 impact mill. The milling parameters were set at a wheel speed of 8000 rpm, airflow of 52 $m^3$/h and feed speed of 20 rpm. The resulting flour was air classified with an ATP50 air classifier at a rotation speed of 2500 rpm, a feed rate of 20 rpm and a 52 $m^3$/h airflow. The final result is that the flour separates into a coarse and fine fraction. The fine fraction

(FF) was used for further fractionation of the proteins. A schematic overview of the fractionation routes is shown in Fig. 1.

#### 2.2.2. Preparation of wet fractionated protein fractions

The fine fraction (FF) was dispersed in water in a 1:10 (w/w) FF/water ratio. While stirring for 2 h, the pH was adjusted to 8.5 using 1 M NaOH solution. Afterwards, the dispersion was centrifugated at 10000 g for 30 min. The supernatant was separated from the pellet and freeze-dried, which resulted in the mildly purified protein mixture (PM). The freshly prepared PM, so not freeze-dried, was further processed by adjusting the pH to 4.5 using 1M HCl, while stirring for 1 h, to induce isoelectric point precipitation. The precipitated proteins were separated by centrifugation at 10000*g* for 30 min. The pellet was re-dispersed in water and the pH was adjusted to 7.0 using 1 M NaOH. After 1 h of stirring, this fraction was freeze-dried to obtain the globulin-rich fraction (GLOB). The supernatant from the acid precipitation step was dialysed against water (using a dialysis membrane with a 3.5 kDa cut-off) at 4 °C to remove the small solutes. The dialysate was changed five times, ensuring the conductivity of the water became constant. Afterwards, the dialysed sample was freeze-dried to obtain the albumin-rich fraction (ALB).

#### 2.2.3. Preparation of the protein colloids

The protein colloids (COL) were prepared using the method from earlier work (Yang et al., 2023). In brief, FF was dissolved in 15 mM sodium metabisulfite solution in a 1:4 (w/w) FF/solution ratio and stirred for 5 min. Afterwards, the pH was adjusted to 8.5 using 1 M NaOH, followed by 1 h stirring. The solution was centrifuged at 10000 g for 30 min, and the supernatant was collected through a paper filter. The pH of the supernatant was adjusted to 6.75 to induce liquid-liquid phase separation. The protein coacervates were heated, while slowly stirring with a magnetic stirrer rod at 80 °C for 20 min, to induce cross-linking. Afterwards, the sample was cooled in an ice-water bath and freeze-dried to obtain the protein colloids (COL).

#### 2.2.4. Determination of protein content

The protein content was analysed using Dumas in a Flash EA 112 NC Analyser (Thermo Fischer Scientific, USA). The nitrogen content was determined and converted into a protein content using a nitrogen conversion factor of 6.25 (Mariotti, Tomé, & Mirand, 2008). All samples were measured in triplicate.

#### 2.2.5. Dissolving samples

All samples were dissolved based on protein content (% w/w) in a 20 mM $PO_4$-buffer, pH 7.0, and stirred for at least 4 h at room temperature. Samples were dissolved in a protein concentration range from 0.1 to 1.0% (w/w), specified in the sections below.

### 2.3. Determination of zeta-potential and particle size

The particle size distribution and zeta-potential were analysed using dynamic light scattering in a Zetasizer Nano ZS (Malvern Instruments Ltd., UK). Solutions with 0.01% (w/w) protein were injected in a DTS1070 Zetasizer cell. The samples were filtered over a 0.45 or 1.2 μm syringe filter (hydrophobic, Whatman) before injection, and the usage of type of filter will be mentioned in the captions. Before analysis, the cell containing the sample was equilibrated for 2 min at 20 °C, followed by a size distribution measurement, where 12 scans were performed in automatic mode, of which an average was calculated. The zeta-potential was determined at 40V with at least 25 single measurements. All measurements were at least performed in triplicate at 20 °C.

### 2.4. Determination of protein size by SEC

Size exclusion chromatography (SEC) was performed using an ÄKTA pure 25 system (Cytiva, Marlborough, MA, USA) equipped with Superdex® 200 10/300 GL column. First, protein solutions with a 0.1% (w/w) protein content were centrifuged at 15000 g for 10 min. The supernatant (50 μL) was injected into the system, and the eluent was a sodium phosphate buffer (20 mM, pH 7.0) containing 50 mM NaCl. The flow rate was set at 0.5 mL/min. The elution was analysed with UV absorbance at 280 nm. A calibration curve was created by running globular proteins with molecular weights ranging from 13.7 to 474 kDa. The calibration curve of standard proteins is provided in Fig. S3 in the SI.

### 2.5. Determination of protein composition by SDS-PAGE

Solutions of 0.1% (w/w) protein were prepared in water. The protein solutions (45 μL) were mixed with NuPAGE LDS sample buffer (7 μL) and 500 mM DDT (6 μL). The mixtures were heated for 10 min at 70 °C and loaded on a 4–12% (w/w) BisTris gel. A Mark 12 molecular weight marker in the range of 2.5–200 kDa was also included. Electrophoresis was performed on the gel for 30 min at 200 V. Afterwards, the proteins were stained with SimplyBlue Safestain, and the gel was analysed using a gel scanner and Image Lab v5.2.1. software.

### 2.6. Determination of protein surface hydrophobicity

The protein surface hydrophobicity was determined using 8-anilino-1-napthalenesulfonic acid ammonium salt (ANSA) as a fluorescence agent. Samples were dissolved in buffer based on protein concentration varying from 0.005 to 0.04% (w/w). Double-sided transparent plastic

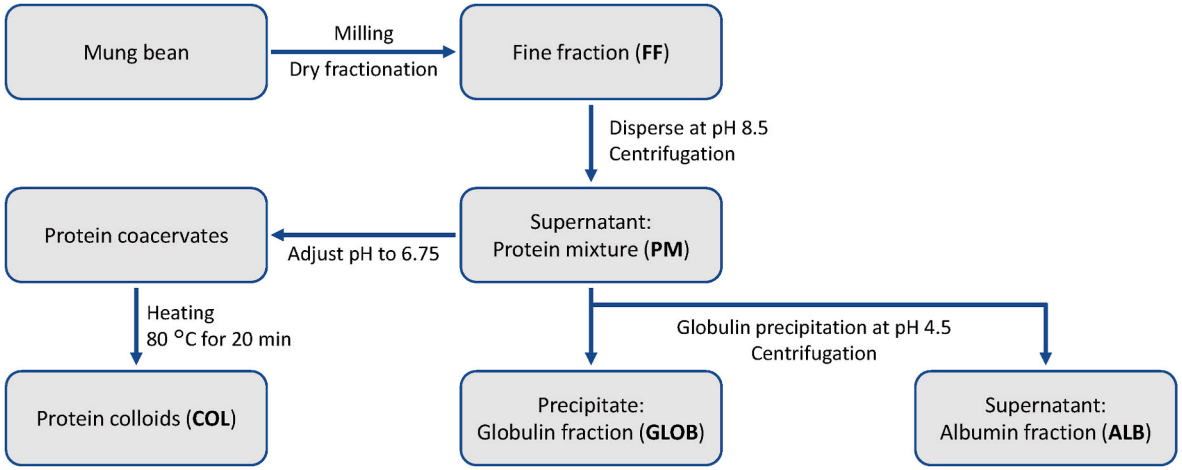


**Fig. 1.** Schematic overview of the protein fractionation routes used to obtain five different protein-enriched fractions.

cuvettes of 4 mL were filled with 3 mL protein solution, and 25 μL of an 8 mM ANSA solution was added. The samples were carefully mixed by rotation and incubated for 1 h in the absence of light to avoid deterioration of the ANSA agent. After incubation, an LS 50B luminescence spectrometer (PerkinElmer, USA) was used, and the excitation wavelength was 390 nm, and the emission wavelength was set at 470 nm. The buffer solution was also included in the analysis as a blank. The slope of the fluorescence intensity over protein concentration was used as a quantification of the surface hydrophobicity. The various samples were compared by calculating a relative surface hydrophobicity among the samples. All samples were analysed in triplicate.

### 2.7. Determination of protein thermal stability by DSC

The protein denaturation properties were determined by a differential scanning calorimetry (DSC) in a Discovery DSC25 (TA Instruments, USA). Stainless steel high-volume pans were filled with about 40 μL of 5% protein (w/w) solutions. An empty stainless-steel high-volume pan was set as a blank reference, and nitrogen was used as a carrier gas. The samples were first equilibrated at 5 °C for 5 min, followed by heating to 140 °C at a rate of 5 °C/min. Subsequently, to investigate potential refolding of the proteins, samples were cooled down from 140 °C to 5 °C at a rate of 10 °C/min, and then reheated to 140 °C at a rate of 5 °C/min. All samples were studied in duplicate.

### 2.8. Determination of surface tension and surface dilatational properties

The mechanical properties of the air-water interface were studied by performing surface dilatational rheology in a drop tensiometer PAT-1M (Sinterface Technologies, Germany). A 0.1% (w/w) protein solution was used to form a hanging droplet with a surface area of 20 $mm^2$ at the tip of a hollow needle. The surface tension was calculated by fitting the Young-Laplace equation to the shape of the droplet. Three types of measurements were performed, and prior to the start of each of these analyses, the droplets were equilibrated for 10800 s. Frequency sweeps were performed at a constant amplitude of 3% and a frequency which increased from 0.002 to 0.1 Hz. Amplitude sweeps were performed at a constant frequency of 0.02 Hz and an amplitude which increased from 3 to 30% deformation. In these oscillatory deformations, five cycles were performed for each frequency or amplitude step. The relaxation behaviour of the interface was also studied by performing step-dilations, where the interface was subjected to a 10% rapid compression or extension (2s step time) of the area. All measurements were performed at least in triplicate at 20 °C.

### 2.9. Rheology data analysis

The raw data of the amplitude sweeps were transformed into Lissajous plots by plotting the oscillating surface stress ($\gamma$-$\gamma_0$) against deformation (($A$-$A_0$)/$A_0$). Here, $\gamma$ and $A$ are the surface tension and area of the deformed interface, $\gamma_0$ and $A_0$ are the surface tension and area of the non-deformed interface. The plots were generated using the middle three oscillations.

### 2.10. Determination of foam properties

#### 2.10.1. Ability and stability of foams created by whipping

Foams were created by whipping 15 mL of 0.1–1.0% protein (w/w) solutions with an overhead stirrer equipped with an aerolatte foam head at 2000 rpm for 2 min in a plastic container (34 mm diameter). The foamability was determined by marking the bottom and upper level of the foam. The height was measured and recalculated into the maximum foam volume using the radius of the container. The foam overrun was defined by:

$$Foam\ overrun\ (\%) = \frac{Maximum\ foam\ volume\ (mL)}{Initial\ solution\ volume\ (15\ mL)}\ x\ 100\% \quad (3)$$

#### 2.10.2. Stability of foams created by sparging

Sparged foams were created in a Foam scan foaming device (Teclis IT-concept, France). A glass cylinder (60 mm diameter) was filled with 40 ml of sample, and gas was sparged through a metal frit (27 μm pore size, 100 μm distance between centres of pores, square lattice) at a flow rate of 400 mL/min. The generated foam in the tube was studied by image analysis to obtain a foam volume, and the foams were sparged to a volume of 400 mL. Afterwards, the foam volume was monitored until a 50% decay of volume, which is known as the foam volume half-life time. A second camera recorded a detailed image of the air bubbles, which was analysed using a custom Matlab script with a DIPlip and DIPimage analysis software package (TU Delft, NL) to determine an average bubble size. All experiments were performed at least in triplicate at 20 °C.

### 2.11. Statistical analysis

The results of this study were shown as means with standard deviation. Statistical analysis was conducted using SPSS v25.0 (IIBM SPSS Inc., USA). One-way ANOVA (one-way analysis of variance) with Duncan post-hoc method ($p < 0.05$) was performed to evaluate the statistical significance of the differences among the means.

## 3. Results and discussion

### 3.1. Protein fractionation process

Dry fractionation of mung bean (MB) resulted in a fine fraction (FF) with 25.2% (w/w) of protein (Table 1). Next to protein, there are still damaged starch granules in the FF present (shown in microscopy images in Fig. S1 in the SI). This was also found for dry fractionated yellow pea seeds, where starch granules were also damaged upon milling (Möller, van der Padt, & van der Goot, 2021). The FF is a fine flour which is next to protein and starch also high in other non-proteinaceous components, such as saccharides (sugars and fibers), phenols and minerals. The remaining starch granules were removed by dispersing the FF in water followed by centrifugation, which yielded the mildly purified protein mixture (PM). Removal of starch was reflected in a protein content increase to 58.8% (w/w) (Table 1). A similar fractionation of yellow pea, which is also a pulse, resulted in a protein content of 54.8% (w/w) (R. Kornet, Yang, Venema, van der Linden, & Sagis, 2022). The remaining 41.2% (w/w) of the PM was previously found to be salts and soluble saccharides for yellow pea (C. Kornet et al., 2020). The PM was further purified by isoelectric point (pI) precipitation at pH 4.5, which resulted in a nearly zero net protein charge of the globulins, leading to aggregation, followed by precipitation. The globulins can be recovered using centrifugation, while non-proteinaceous solutes are removed, leading to a globulin-rich fraction (GLOB) with a protein content of 89.4% (w/w).

**Table 1**
The protein content (Nx6.25) based on dry matter (% w/w) and protein recovery (expressed as the amount of protein obtained from the FF) of FF (fine fraction), PM (protein mixture), COL (protein colloids), GLOB (globulin fraction), and ALB (albumin fraction). Values are presented as mean ± standard deviation. The values with the same superscript are not significantly different ($p > 0.05$) from each other.

| | Protein content (%) | Protein recovery (%) |
|---|---|---|
| FF | $25.2 \pm 0.4^{a}$ | 100.0 |
| PM | $58.8 \pm 3.2^{c}$ | 79.4 |
| GLOB | $89.4 \pm 0.6^{d}$ | 66.6 |
| ALB | $47.1 \pm 1.5^{b}$ | 10.5 |
| COL | $50.0 \pm 0.5^{b}$ | 80.0 |

A drawback of extensive purification is a lower protein recovery of 66.6% (w/w), while PM had a protein recovery of 79.4% (w/w). The major difference is the loss of albumins in the supernatant after the isoelectric precipitation step, as albumins remain soluble at a large pH range between 2 and 12 (González-Pérez et al., 2005). Direct utilisation of the albumin-rich supernatant has a potential drawback, as many non-protein components are present, such as salts, saccharides, but also anti-nutritional components, such as lipoxygenases, phytic acids and tannins (Chua & Liu, 2019). However, these solutes were removed using dialysis (or filtration), leading to the albumin-rich fraction (ALB) with a protein content of 47.1% (w/w). The protein colloid fraction had a protein content of 50.0% (w/w). Based on protein purity, we show how more intense fractionation led to higher protein contents, but lower protein recovery values. For a fair comparison, we standardised all solutions on protein content.

### 3.2. Protein composition

In the next step, the protein composition was analysed using SDS-PAGE under reducing conditions, where disulphibe bonds between protein subunits were broken down (Fig. 2A). The two major storage protein classes globulin and albumin can be observed in the gel. Globulins in legumins are further divided into two sub-classes: vicilin (VIC) and legumin (LEG) (Mendoza, Adachi, Bernardo, & Utsumi, 2001; Tang & Sun, 2010). Native MB vicilin had a molecular weight between 158 and 200 kDa, while MB legumin had a molecular weight of around 360 kDa. For GLOB, there are high-intensity bands between 20 and 30 kDa, at 34 kDa, and between 40 and 55 kDa. Subunits for legumin were previously identified at 24 and 40 kDa, while vicilin had subunits at 26, 32, 48 and 60 kDa (Mendoza et al., 2001). A majority of these bands are prominently present on the lanes of FF, PM, and GLOB, indicating the presence of both MB vicilin and legumin.

A few typical bands were found for albumins at 25 kDa and between 70 and 95 kDa. The FF and PM had bands for globulin and albumin subunits, which is expected as FF is unprocessed (obtained after dry fractionation), and both proteins are retained in PM due to the mild wet fractionation method. Similar protein composition was also found when performing size exclusion chromatography (SEC) on FM and PM (data shown in Fig. S2 in the SI). The GLOB showed thicker bands for the globulin subunits, and the bands for albumin proteins were (nearly) absent. The opposite was observed for the ALB sample, suggesting a successful separation of both albumin and globulins. The separation of albumin and globulin from PM into ALB and GLOB was again confirmed using SEC (Fig. 2B). Here, prominent peaks for legumin (11 min elution time, 660 kDa) and vicilin (12 min, 258 kDa) are present in GLOB, and absent in ALB. The ALB sample showed dominating peaks at 14.5 (113 kDa) and 17 min (32 kDa), showing the major fraction in this isolate are albumins. Also here, the smaller size of albumins compared to globulins (legumin & vicilin) is evident.

COL showed both bands for albumins and globulins in the SDS-PAGE gel (Fig. 2A), but the bands had lower intensity compared to PM. Fewer proteins might be incorporated in the gel, as the proteins are expected to form large colloids in COL that might not have passed into the much smaller pores of the gel. We will evaluate the particle size of the MB protein fractions in the next section.

### 3.3. Protein size distribution

Size distributions of the MB protein fractions obtained from dynamic light scattering are shown in Fig. 3. The FF had a peak between 100 and 220 nm with a maximum peak height at 164 nm, which are probably protein bodies or starch granule fragments. Large starch granules are not shown in the size distribution of FF, as the sample was filtered over 1.2 μm before analysis. Of course, smaller albumin and globulin proteins might be present in FF, but the peak at 100–220 nm is most likely dominating the overall scattering signal. This material was removed when creating the PM fraction, which showed a peak at a smaller size between 4 and 20 nm with a maximum peak height at 10 nm. GLOB

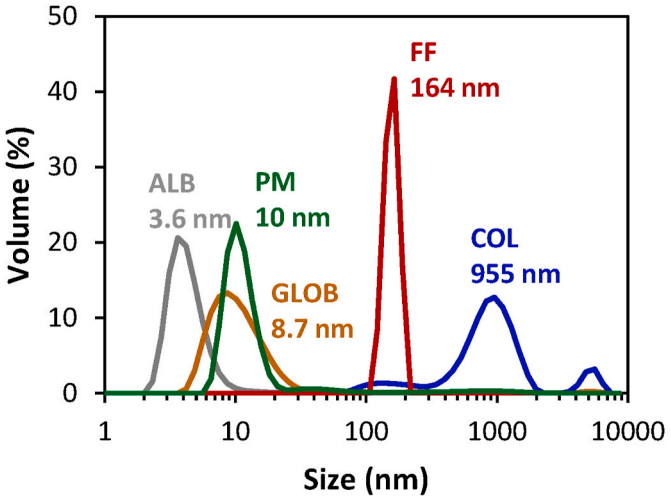


**Fig. 3.** The size distribution of MB protein fractions: FF (fine fraction, filtered over 1.2 μm), PM (protein mixture, filtered over 0.45 μm), COL (coacervate colloids, unfiltered), GLOB (globulin fraction, filtered over 0.45 μm), and ALB (albumin fraction, filtered over 0.45 μm). The peak protein sizes are included in the graph. For clarity reasons, one representative measurement is shown for each sample, while comparable results were obtained from three replicates.

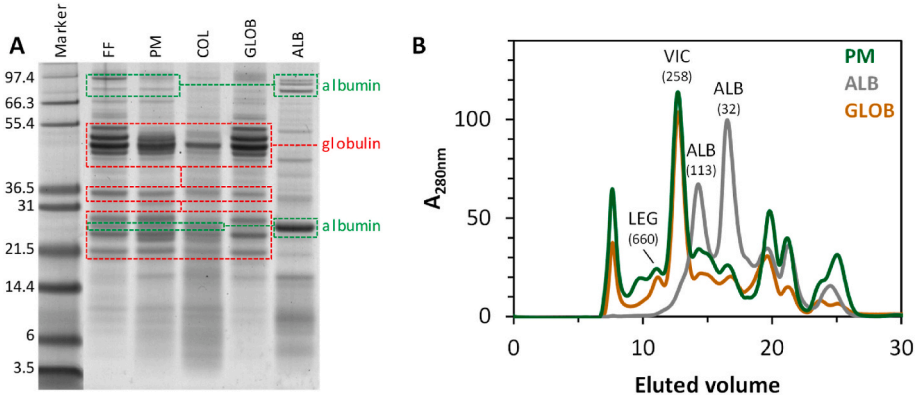


**Fig. 2.** (A) SDS-PAGE profile under reducing conditions of FF (fine fraction), PM (protein mixture), COL (protein colloids), GLOB (globulin fraction), and ALB (albumin fraction). (B) SEC chromatogram with the 280 nm absorbance over eluted volume of PM, ALB and GLOB. The numbers in brackets indicate the molecular weight (kDa) of the corresponding peak. The calibration curve can be found in the SI.

showed a comparable size distribution with a similar peak at 8.7 nm, while ALB had a peak at 3.6 nm. A smaller size for ALB is expected as albumins are smaller than globulins, as shown in the SDS-PAGE profile & SEC chromatogram (Fig. 2). Also, the globulins seem to dictate the size distribution of PM, which could be due to the presence of more globulins than albumins. Based on the protein yield, we expect roughly 13% of albumins and 87% globulins in the PM. Finally, the COL was substantially larger, with a major peak between 400 and 2000 nm. This confirms the formation and presence of protein colloids.

### 3.4. Protein heat denaturation properties

Extensive purification or processing of proteins might alter the protein structure. Therefore, the protein thermal properties were evaluated using differential scanning calorimetry (DSC). The denaturation temperatures and enthalpy are shown in Table 2. FF had lower denaturation temperatures ($T_{onset}$ and $T_{peak}$ of 70.8 and 76.6 °C) compared to PM, and also a substantially higher enthalpy (30.2 J/g) due to starch gelatinisation (Hoover et al., 1997). PM (obtained through removal of starch) had a $T_{onset}$ and $T_{peak}$ of 72.6 and 80.7 °C, respectively. The denaturation behaviour of PM is most likely dominated by the globulins, as GLOB showed comparable denaturation temperatures, while albumin showed lower ones. However, the denaturation enthalpy of GLOB is about 23% lower compared to PM. One could argue that the GLOB fractionation might have altered protein structure, such as increased aggregation, as also found for pea globulins (C. Kornet et al., 2020). This could ultimately lead to the slightly lower enthalpy of GLOB.

ALB had a substantially lower enthalpy than GLOB, which is related to their tertiary protein structures. From other plant sources, it is known that globulins are folded into (larger) globular structures, while albumins have a more simple structure (Gonzalez-Perez & Vereijken, 2007; Souza, 2020). COL had the highest denaturation temperatures, which was expected, as the sample was heated at 80 °C. Even though 80 °C is at the peak denaturation temperature of the globulins, complete denaturation of proteins requires higher temperatures. We expect that a portion of the globulins is not or only partly denatured, which is reflected in the remaining denaturation enthalpy of 3.4 J/g protein for COL. In summary, the extensive purification process to obtain GLOB and ALB seemed to slightly alter the protein nativity of the globulins, while heating the colloids resulted in vast alteration of protein structure.

### 3.5. Protein surface hydrophobicity and zeta-potential

The protein surface properties (influenced by hydrophobicity and charge of the protein) are known to affect the protein's interfacial properties. Therefore, we evaluated the relative protein surface hydrophobicity (Table 3). In previous studies, globulins of yellow pea, Bambara groundnut and rapeseed were found to have a higher surface hydrophobicity than albumins (C. Kornet et al., 2020; Ntone et al., 2021; J. Yang, de Wit et al., 2022). A similar relationship is present in this work, as the surface hydrophobicity of GLOB is about 45% higher than ALB. FF and PM showed lower surface hydrophobicity, which could be related to the presence of non-proteinaceous components that cover hydrophobic domains of the protein or interfere with the hydrophobic probe. Another explanation is the slight alteration of protein structure due to the extensive processing, as shown by DSC (Table 2). This could lead to higher surface hydrophobicity values for GLOB and ALB in comparison to FF and PM. The highest surface hydrophobicity was found for COL, which is between 3 and 10 times higher than the other MB protein fractions. This finding is not unexpected, as the COL sample was heat-denatured to form cross-links, thus leading to more exposed hydrophobic groups on the surface of the coacervate colloids. A second protein surface property of interest is the zeta potential (Table 3). Here, we showed a zeta-potential between −14.8 and −22.4 mV for FF, PM, GLOB and COL. These fractions are high in globulins, which probably resulted in comparable surface charges. Albumins showed a substantially lower zeta-potential of −2.3 mV.

**Table 2**
Protein denaturation temperature and enthalpy of MB protein fractions. Values are presented as mean ± standard deviation.

| | FF | PM | GLOB | ALB | COL |
|---|---|---|---|---|---|
| $T_{onset}$ (°C) | 70.8 ± 0.8 | 72.6 ± 0.0 | 71.2 ± 0.9 | 67.6 ± 0.3 | 80.7 ± 0.0 |
| $T_{peak}$ (°C) | 76.6 ± 0.1 | 80.7 ± 0.1 | 79.4 ± 0.9 | 76.6 ± 0.1 | 87.6 ± 0.1 |
| Enthalpy (J/g protein) | 30.2 ± 1.0 | 10.4 ± 0.2 | 8.0 ± 0.0 | 2.7 ± 0.0 | 3.4 ± 0.1 |

**Table 3**
The relative protein surface hydrophobicity and zeta-potential of FF (fine fraction), PM (protein mixture), COL (protein colloids), GLOB (globulin fraction), and ALB (albumin fraction) in 20 mM $PO_4$ buffer, pH 7.0. Values are presented as the mean value ± standard deviation. The means with the same superscript in the same column are not significantly different from each other ($p > 0.05$).

| | Relative protein surface hydrophobicity | Zeta-potential (mV) |
|---|---|---|
| FF | $0.18 \pm 0.01^{b}$ | $-22.4 \pm 2.3^{a}$ |
| PM | $0.10 \pm 0.01^{a}$ | $-19.8 \pm 1.8^{a}$ |
| GLOB | $0.29 \pm 0.02^{c}$ | $-14.8 \pm 0.9^{b}$ |
| ALB | $0.20 \pm 0.02^{b}$ | $-2.3 \pm 1.5^{c}$ |
| COL | $1.00 \pm 0.04^{d}$ | $-19.7 \pm 1.6^{a}$ |

### 3.6. Interfacial properties

#### 3.6.1. Adsorption behaviour

All the samples showed an immediate increase of surface pressure at the first measurement point at 1 s (Fig. 4A). ALB had the highest initial surface pressure increase. The rapid initial adsorption of ALB probably results from the small molecular size, leading to a high diffusional flux towards the interface. The smaller size and low surface charge of albumins can also contribute to a lower energy barrier for adsorption. GLOB showed a much slower initial adsorption compared to ALB, probably due to the higher molecular weight and surface charge. FF and PM showed higher surface pressure values over the 3 h of adsorption time. This could be a contribution of albumins for FF and PM, as both albumins and globulins are present. We should also keep in mind that many non-proteinaceous components (e.g. phospholipids and phenols) are present in FF and PM, which can compete with the proteins for the interface, or interact with the proteins, thereby affecting the surface properties of the proteins (Bock, Steinhäuser, & Drusch, 2021; He et al., 2008). This might explain the higher surface activity of FF and PM compared to GLOB.

The protein colloids (COL) showed a slight surface pressure increase in the initial phase (first 20 s) compared to GLOB, which is surprising, as the protein colloids are much larger (Fig. 3). Such large colloids (400–2000 nm) are not expected to adsorb at the air-water interface due to the high energy barrier against adsorption. In previous work, whey protein colloids were produced, which also did not adsorb at the air-water interface (Yang, Thielen, Berton-Carabin, van der Linden, & Sagis, 2020), while smaller non-cross-linked material also present in the dispersion dictated the interfacial properties. For the COL fraction, we also expect the interfacial dominance of non-cross-linked proteins, which might be highly surface-active due to exposure of hydrophobic groups, as shown in the surface hydrophobicity determination (Table 3).

#### 3.6.2. Surface dilatational rheology

The mechanical properties of air-water interfacial films stabilised by the MB protein fractions were studied using surface dilatational rheology. Frequency and amplitude sweeps, and step-dilatations were performed.

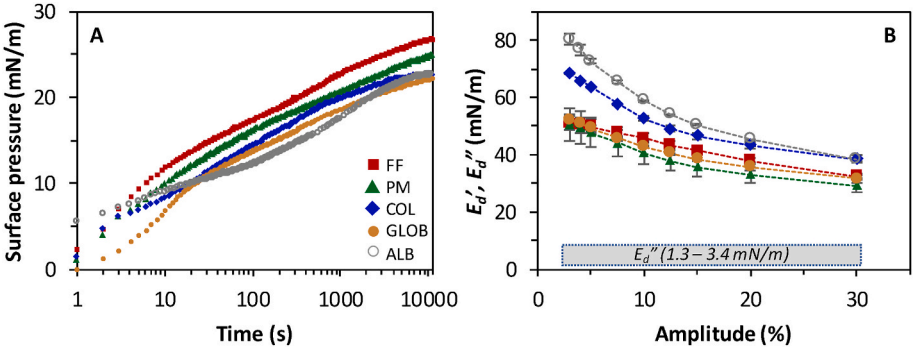


**Fig. 4.** (A) The surface pressure as a function of time of FF (fine fraction), PM (protein mixture), COL (coacervate colloids), GLOB (globulin fraction), and ALB (albumin fraction). Averages of three replicates are shown, and the standard deviation was below 5%. (B) The surface dilatational moduli versus deformation amplitude of the earlier mentioned MB protein fractions. The $E_d$' was shown as symbols with a line to guide the eye, while the Ed" of all samples were very low, with values in the grey area. The shown averages and standard deviations are the results of at least three replicates.

*3.6.2.1. Frequency sweeps.* In frequency sweeps, the deformation amplitude was constant at 3%, while the frequency of the oscillation was varied. The dilatational storage moduli (results not shown) showed a weak power law dependence on frequency, i.e., $E_d' \sim \omega^n$. The n-values are shown in Table 4. An n-value of 0.5 was previously related to an interfacial film, where the elasticity is determined by the mass exchange of stabiliser between the bulk and the interface, also known as the Lucassen-Van den Tempel model (Lucassen & van den Tempel, 1972). The interfacial layers stabilised by the different MB protein fractions had n-values between 0.08 and 0.17. The storage modulus was significantly higher than the loss modulus, typical for soft viscoelastic disordered solids [43,45]. Exchange of material between bulk and interface does not appear to play a significant role in the response, which is more likely governed by in-plane rearrangements and momentum exchange with the bulk phase.

*3.6.2.2. Amplitude sweeps.* The mechanical properties of the interfacial films were further analysed by performing amplitude sweeps, where the deformation amplitude of the interfacial area is increased from 3 to 30%, while the oscillation frequency is constant (Fig. 4B). Here, we are interested in the magnitude and amplitude dependence of the surface dilatational elastic moduli $E_d$'. When comparing ALB- and GLOB-stabilised interfaces, the ALB had higher moduli decreasing from 80 to 38 mN/m, while GLOB had lower moduli between 52 and 32 mN/m. This implies the formation of stiffer layers by ALB. The lower amplitude dependence of GLOB indicates there is less disruption of the surface microstructure compared to ALB. The FF- and PM-stabilised interfacial films had moduli of 51–32 and 51–29 mN/m, respectively, similar to GLOB. This would indicate a globulin-dominated interfacial layer for FF and PM, probably due to the high concentration of globulins. The moduli of COL were between those of GLOB and ALB, with a decrease from 68 to 38 mN/m. That COL formed stiffer interfacial layers than GLOB, FF and PM could be related to the increased hydrophobic interactions among adsorbed proteins (see Table 3).

The microstructure of the interfaces was clearly affected by large deformations, as the $E_d$' values (Fig. 4B) decreased with increasing deformation amplitudes, also known as nonlinear viscoelastic (NLVE) behavior. Disruptions of the interfacial microstructure can lead to nonlinearities in the surface stress/pressure signal. The moduli in Fig. 4 are obtained by Fourier transforming the surface stress signal and calculated using the intensity and phase of the first harmonic of the obtained Fourier spectrum. Using the first harmonic is reliable only when the deformations are small and in the linear viscoelastic (LVE) regime, where nonlinearities are negligible. Most of the deformations in Fig. 4B are in the NLVE regime, leading to nonlinearities, thus higher-order harmonics in the Fourier spectrum. These higher-order harmonics (and nonlinearities) are neglected in the $E_d$' calculation. A qualitative analysis method to incorporate the nonlinearities is plotting the surface pressure as a function of deformation in Lissajous(-Bowditch) plots (Ewoldt, Hosoi, & McKinley, 2007; Xia, Botma, Sagis, & Yang, 2022).

**Table 4**
The n-value of $E_d' \sim \omega^n$, obtained from frequency sweeps on MB-protein stabilised interfacial films. Values are presented as mean ± standard deviation.

| | n-value |
|---|---|
| FF | $0.17 \pm 0.02^b$ |
| PM | $0.14 \pm 0.03^b$ |
| COL | $0.08 \pm 0.03^a$ |
| GLOB | $0.16 \pm 0.03^b$ |
| ALB | $0.14 \pm 0.02^b$ |

*3.6.2.3. Lissajous plots.* Lissajous plots of the MB-protein fraction-stabilised interfaces are shown in Fig. 5. The plots move clockwise, where the interfacial area is extended in the upper part of the cycle, and the opposite (compression) occurs in the bottom part of the cycle. An important characteristic is the width of the plots, which indicates the type of rheological response of the interfacial layer. A straight line (closed plot) reveals a fully elastic response, a circle indicates a viscous response, and an ellipse suggests a viscoelastic response. The angle of the main axis of the plots with the horizontal axis is related to the interfacial stiffness, and a plot that is more tilted towards the vertical axis suggests a stiffer interface. Nonlinearities can lead to asymmetries between the extension and compression cycle, which we will elaborately discuss for the graphs.

At 5% deformation, the COL- and ALB-stabilised interfaces showed wider plots compared to FF, PM and GLOB. This indicates a higher energy dissipation upon deformation. Also, the COL and ALB are more tilted toward the vertical axis, indicating a stiffer interfacial film. Nonlinear behaviour was clearly present at 30% deformation, as all plots become asymmetric. For both COL and ALB, at the start of the extension part of the cycle (bottom-left point), we can observe a relatively fast surface pressure increase, followed by a gradually smaller increase of surface pressure. For COL, a nearly flat curve can be observed between a deformation of 0.25–0.30. Such behaviour is called intra-cycle strain softening in extension, revealing a gradual disruption (and softening) of the microstructure. With this, the elastic component of the response diminishes, while the viscous component starts dominating. On the time scale of a single cycle, there was negligible mass transfer between bulk and interface (as evident from the frequency sweeps). This means the surface density decreases upon expansion, and this may also contribute to the observed softening behaviour.

In the compression cycle, we can observe an opposite phenomenon, as the surface pressure rapidly decreases to values of −18 and −20 mN/m at a deformation of −0.35 for ALB and COL. This behaviour is known as intra-cycle strain hardening in compression, as the adsorbed proteins are concentrated upon (extensive) compression, resulting in the jamming of proteins at the interface. The combination of strain softening in extension and strain hardening in compression implies strong in-plane interactions between adsorbed proteins. Such behaviour was

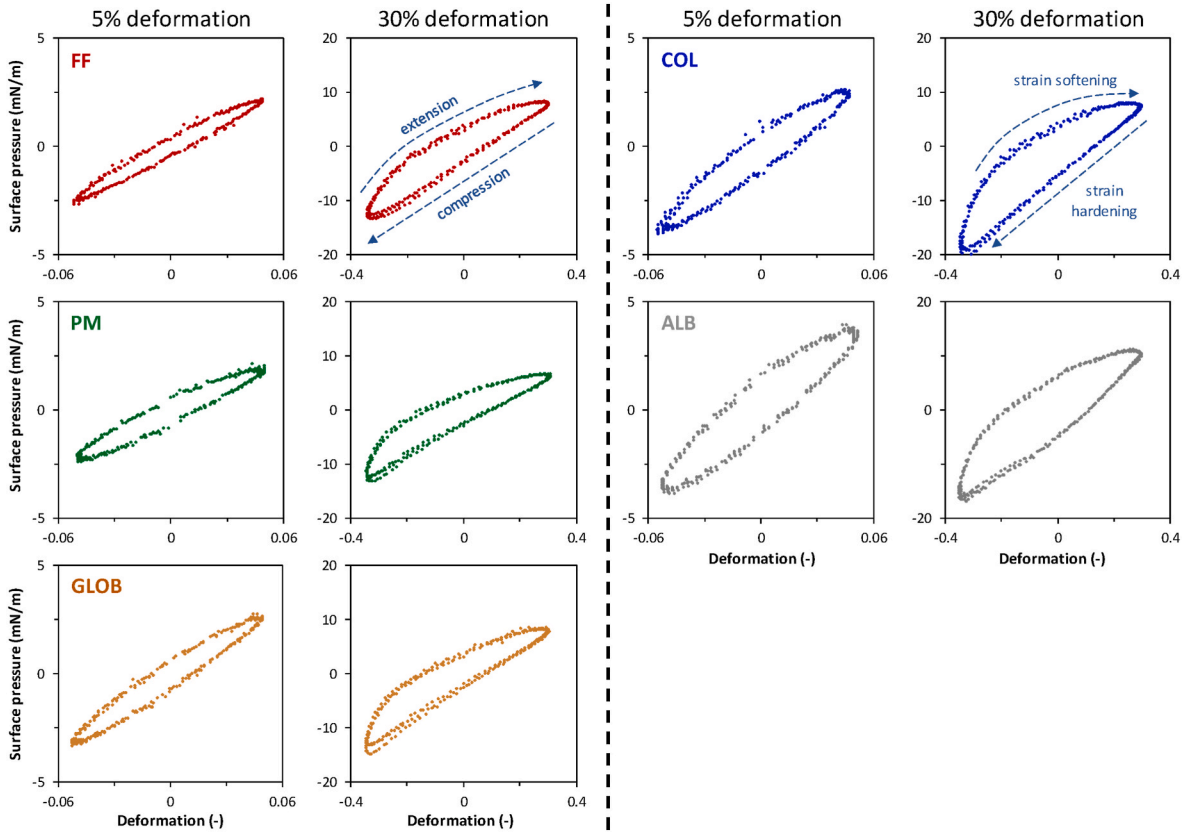


**Fig. 5.** Lissajous plots of surface pressure as a function of deformation. The plots are obtained from the amplitude sweeps of interfacial layers stabilised by the MB protein fractions: FF (fine fraction), PM (protein mixture), COL (coacervate colloids), GLOB (globulin fraction), and ALB (albumin fraction). One representative plot is shown for each sample, while comparable plots were obtained for at least three replicates.

previously related to the formation of viscoelastic solid-like interfacial layers (Hinderink, Sagis, Schroën, & Berton-Carabin, 2020; Yang et al., 2020). The ability of albumins to form stiff solid-like interfacial layers was previously related to the small molecular size and low surface charge (Yang, Kornet, et al., 2022). This would allow a closer approach of proteins and more effective coverage, leading to stronger in-plane protein-protein interactions. The proteins in the COL might be able to form such layers due to the high surface hydrophobicity (Table 3), which can also lead to stronger attractive interaction.

Different behaviour is observed for the FF-, PM- and GLOB-stabilised interfaces, as these protein fractions show narrower 5% deformation plots that are more tilted towards the horizontal axis. At 30%, the asymmetries were less pronounced in comparison to the ALB- and COL-stabilised interfaces. This implies that the FF-, PM- and GLOB-stabilised interfaces formed weak and more easily stretchable interfaces. We also conclude that the globulins dominate the interfacial properties in both FF and PM, which was also observed for a protein mixture from yellow pea and Bambara groundnut (Kornet et al., 2022; Yang, de Wit et al., 2022). For Bambara groundnut, it was shown explicitly that the legumin dominated the interfacial properties in a globulin mixture of both legumin and vicilin, probably due to faster adsorption of legumin at the air-water interface than vicilin. The weak interfacial layers formed by MB globulin could be due to their largely aggregated state in combination with high surface charges. As a result, this could lead to a lower and less effective surface coverage, thus weaker in-plane interaction at the interface. The globulins seem to dominate the FF-, PM- and GLOB-stabilised interfaces, as comparable rheological behaviour is shown, which also suggests that the non-proteinaceous material (e.g. phospholipids and phenols) play a limited role in the interfacial network formation.

*3.6.2.4. Step-dilatation experiments.* The interfacial properties of the MB protein fraction-stabilised interfaces were further investigated by studying the relaxation response. The response was initiated by performing step-dilatations on the air-water interface. The relaxation response was fitted with a combination of a Kohlraus-William-Watts (KWW) stretch exponential and a regular exponential term (Equation (1)) (Watts & Davies, 1969).

$$\gamma(t) = ae^{-(t/\tau_1)^{\beta}} + be^{-t/\tau_2} + c \quad (1)$$

Here, the stretch exponent β and relaxation time $\tau_1$ are shown in Table 5. Other parameters, such as the characteristic time of the second term $\tau_2$ and fitting parameters a, b, and c are shown in Table S1 in the SI. The KWW is a phenomenological model that was initially used to describe the relaxation responses of disordered systems and later for protein-stabilised interfaces (Klafter & Shlesinger, 1986; Sagis et al., 2019; Watts & Davies, 1969; Yang et al., 2021). A stretch component of $\beta < 1$

**Table 5**
The stretch exponent β and characteristic relaxation time $\tau_1$ values obtained from step-dilatation experiments of air-water interfaces stabilised by the MB protein fractions. Values are presented as mean ± standard deviation. The means with the same superscript in the same column are not significantly different from each other ($p > 0.05$).

| | Extension | | Compression | |
|---|---|---|---|---|
| | β | T1 (s) | β | T1 (s) |
| **FF** | $0.60 \pm 0.03^{a}$ | $32.4 \pm 6.9^{b}$ | $0.58 \pm 0.01^{a}$ | $27.9 \pm 7.1^{ab}$ |
| **PM** | $0.60 \pm 0.02^{a}$ | $30.8 \pm 8.4^{a}$ | $0.59 \pm 0.03^{a}$ | $23.8 \pm 4.0^{ab}$ |
| **COL** | $0.57 \pm 0.04^{a}$ | $25.2 \pm 5.1^{a}$ | $0.63 \pm 0.04^{a}$ | $34.1 \pm 8.2^{b}$ |
| **GLOB** | $0.54 \pm 0.05^{a}$ | $22.2 \pm 3.7^{a}$ | $0.60 \pm 0.06^{a}$ | $17.3 \pm 5.3^{ab}$ |
| **ALB** | $0.53 \pm 0.03^{a}$ | $19.2 \pm 8.0^{a}$ | $0.60 \pm 0.05^{a}$ | $18.1 \pm 3.5^{ab}$ |

indicates dynamic heterogeneity, which may suggest a wide range of relaxation times due to local variations in the relaxation response. In our work, we show β values varying from 0.53 to 0.63 for all MB protein-stabilised interfaces. This reveals the presence of dynamic heterogeneity, which we previously related to the heterogeneous microstructure of a protein-stabilised interface (Yang et al., 2020). Such a microstructure is comprised of proteins clusters, leading to the co-existence of dilute/dense and thicker/thinner regions. Such dissimilarities could result in local differences in the relaxation response, thus a wide range of relaxation times, and the emergence of dynamic heterogeneity. The relaxation time varies between 19.2 and 34.1 s, which is typical for protein interfaces (Sagis et al., 2019). The relaxation response of these interfacial films indicates the formation of disordered/heterogeneous solid-like materials, as observed for a wide range of protein-stabilised interfacial films (Kornet et al., 2022; Rühs, Affolter, Windhab, & Fischer, 2013; Yang et al., 2020). The findings from the step-dilatation experiment, in combination with the frequency and amplitude sweeps demonstrate the formation of viscoelastic disordered solid-like interfacial films by the MB fractions.

### 3.7. Foams

#### 3.7.1. Foamability

The foamability of the MB protein-stabilised foams was evaluated by studying the foam overrun after whipping, and the average air bubble size after sparging with nitrogen gas (Fig. 6A and B). The overrun was determined as the foam volume expressed over the initial protein solution volume. The FF, PM and GLOB, where the globulins dominated the interfacial properties, had the lowest overruns. These values were 58, 76 and 42% at 0.1% (w/w) and 222, 258 and 200% at 1.0% (w/w) protein for FF, PM and GLOB, respectively. A substantially higher overrun was found for the ALB with values of 307 and 342% at 0.1 and 1.0%, respectively. At 0.1% (w/w) protein, the globulin-dominated fractions (FF, PM and GLOB) also had much larger air bubble sizes (0.39, 0,34 and 0,20 mm) than ALB (0.06 mm). Albumins formed higher volumes of foam with smaller air bubbles, which is in line with the initially faster adsorption of ALB compared to FF, PM and GLOB (Fig. 4A). The ability to form stiffer interfacial layers by ALB also contributes to a higher foam volume, as the air bubbles are protected against immediate coalescence during foam formation, leading to more and smaller air bubbles, thus higher foam volumes. Another major parameter that can affect foaming properties is the protein solubility. For the fractions discussed in this section, we expect >85% solubility, as shown in previous work for yellow pea (also a legume), which were extracted using similar fractionation methods (Kornet et al., 2020). The COL have a solubility of 68% at pH 7.0 (Yang et al., 2023).

At 1.0% (w/w) protein, the PM-stabilised foam had the smallest air bubbles (0.06 mm) and hightest overrun (258%) among the globulin-dominated fractions (FF, PM and GLOB). PM is comprised of both albumins and globulins. The albumins in PM might have contributed to the increased foamability. The FF also contains albumins but has the largest air bubbles. The large starch granules present in this fraction could act as anti-foaming particles during foam formation. Solid particles may rupture thin films by a mechanism called bridging dewetting (Denkov & Marinova, 2006). Here, the particle is present between two films, and will contact both films upon thinning due to drainage. The particle may dewet the liquid, resulting in the thin film's perforation, and finally, film rupture. As a result, bubbles coalesce, leading to lower foam overrun.

#### 3.7.2. Foam stability

The foam stability was determined from the foam half-life time, which is the time required for the foam volume to decay by 50% (Fig. 6C). The bulk viscosity of the solution can increase foam stability, as higher viscosity might decrease liquid drainage. Therefore, the viscosity of the protein solutions was analysed, which was found to be close

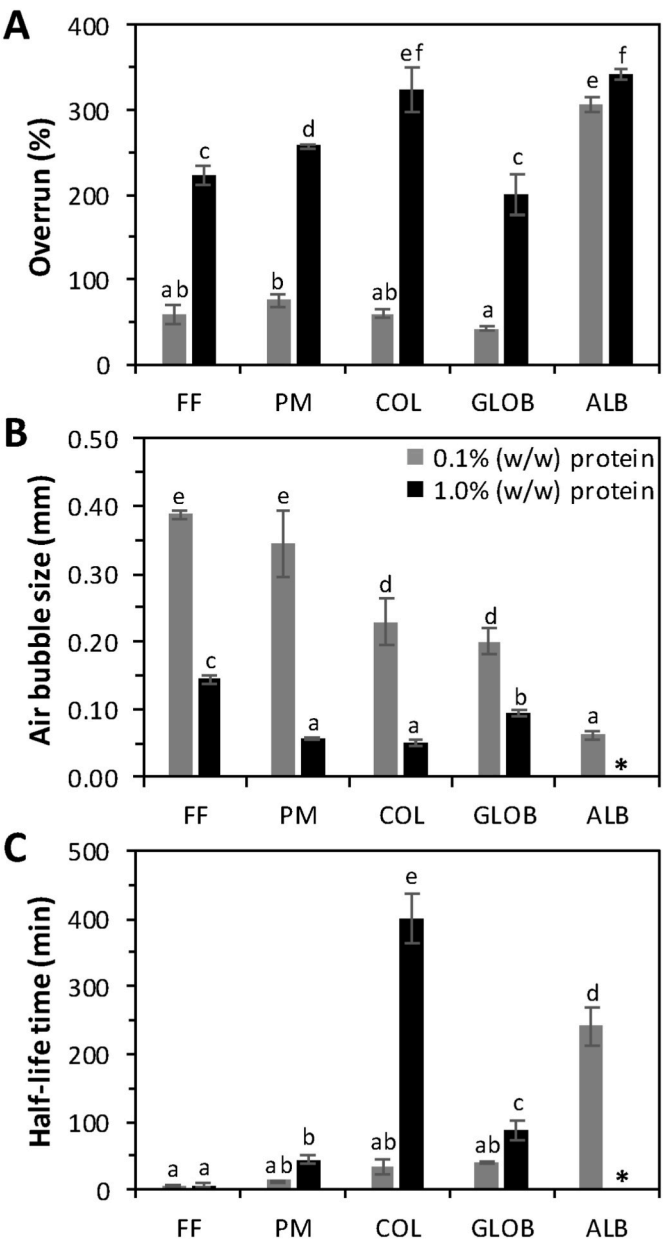


**Fig. 6.** (A) The overrun, (B) average air bubble size directly after foam formation, (C) volume half-life time of foams prepared with FF (fine fraction), PM (protein mixture), COL (coacervate colloids), GLOB (globulin fraction), and ALB (albumin fraction). Foams were created at 0.1% and 1.0% (w/w) protein, shown in grey and black bars, representatively. The averages and standard deviations are the results of at least three replicates. □ = 1.0% (w/w) albumin foams were not created for air bubble size and half-life time analysis.

to that of water for all samples (shown in Table S2 in the SI). Therefore, the bulk viscosity is not able to explain the differences in the foaming properties of the different protein fractions.

The FF had the lowest half-life times (below 6 min), which is most likely due to destabilisation by starch granules. Removal of granules results in PM, with higher foam stability and a half-life time up to 45 min at 1.0% (w/w). GLOB had an even longer half-life time of 87 min at 1.0% (w/w) protein. The higher foam stability of GLOB compared to PM would suggest that the non-proteinaceous components in PM (e.g. phospholipids and phenols) reduced the stability. ALB had substantially higher foam stability with a half-life time of 240 min at 0.1% (w/w), which is probably the result of the formation of smaller air bubbles and stiffer interfacial layers. The smaller and monodisperse distribution of

air bubbles reduces the rate of disproportionation, and the stiffer interfacial layers also reduce the rate of disproportionation and the probability of air bubbles coalescence. As shown in previous studies, plant albumins formed stable foams due to their small molecular size and low surface charges, while the highly aggregated globulins resulted in larger air bubbles and weaker interfacial films, thus lower foam stability (Ghumman, Kaur, & Singh, 2016; Lu, Quillien, & Popineau, 2000; Yang, Kornet, et al., 2022).

Interestingly, the foam stability of PM did not increase due to the presence of albumins, while the foamability was slightly higher for PM (in comparison to GLOB). We could argue that the total amount of albumins is too low, only comprising ~13% of the total protein content in PM (calculated based on protein yield in the current work). The albumins might contribute to the formation of more interfacial area, thus smaller air bubbles and higher foam volumes. However, globulins seem to dictate the mechanical properties of the PM-stabilised air-water interface, as shown by interfacial rheology (Fig. 5), which could result in lower foam stability of PM. Of course, here we should again not forget the presence of non-proteinaceous components in the PM, which are most likely present at the interface, as shown by the higher surface pressure of PM compared to GLOB in Fig. 4A. With regard to the extent of purification, the FF-, PM- and GLOB-stabilised foams showed similar foamability. It seems that no or mild purification is sufficient to obtain a foaming ingredient with good foamability. However, more extensive purification does result in higher foam stability, most likely by removal of non-proteinaceous foam destabilisers, such as starch granules, phenols and phospholipids. Besides, the side stream of the extensive process (ALB) possesses superior foaming properties. It is worth mentioning that the foaming properties of the ALB were nearly as good as whey protein isolate-stabilised foams, which had a foam half-life time of 258 min (Yang, Kornet, et al., 2022), while ALB had one of 240 min at a similar protein concentration and system conditions (method of foam formation and dissolution buffer).

#### 3.7.3. Foaming properties of protein colloids

A final sample in this study are the protein colloids (COL). At 0.1% (w/w) COL showed a foam overrun of 60%, similar to FF, PM and GLOB (Fig. 6A). At 1.0% (w/w), the overrun increased vastly to 324%, nearly as high as ALB. As mentioned in earlier sections, we expect the small non-cross-linked proteins to dominate the interfacial properties of COL. With this in mind, the absolute amount of surface active non-cross-linked proteins is low at 0.1% (w/w), but increases by tenfold at 1.0% (w/w). This was also reflected in the average air bubble size (Fig. 6B), which was found to be 0.05 mm, even smaller than air bubbles of 1.0% (w/w) PM-stabilised foams. The most prominent improvement is the foam stability, with a half-life time of 400 min at 1.0% (w/w). Turning PM into COL resulted in a foam stability increase of roughly 12 times. The high foam stability could result from the formation of stiff interfacial layers, as shown in interfacial rheology (Fig. 5). In addition, the colloids could also contribute to the foam stability, as particles can cause pinning in the foam. In this process, the colloids are trapped in the lamellae and plateau borders between the air bubbles. This process can vastly reduce the drainage and increase thin film stability, thus slowing down the coalescence of air bubbles. Such a phenomenon was previously shown for casein particles and dairy protein aggregates (Chen et al., 2017; Dhayal et al., 2015; Rullier et al., 2008). In conclusion, the formation of coacervate colloids can improve the low foam stability of PM, even though non-proteinaceous components are present. It is a promising and controlled method to significantly enhance the foaming properties of mung bean proteins.

## 4. Conclusions

In this work, the physical-chemical, interface and foam stabilising properties of five mung bean protein fractions were evaluated. The interfacial properties of the dry fractionated fine fraction (FF), the protein mixture (PM) and globulin-rich fraction (GLOB) were similar, suggesting that globulins dominated the interfacial films for FF and PM. Physical-chemical analysis showed large (and aggregated) globulin proteins with high zeta-potential. This could lead to an ineffective surface coverage with weak in-plane protein-protein interactions. As a result, the globulin proteins formed weak and more easily stretchable interfacial layers, leading to low foamability and stability for FF, PM and GLOB.

The other major protein in mung bean are the albumins (ALB), which are smaller proteins with lower zeta-potential values. This may lead to higher protein surface density, giving a stiff interfacial film due to strong protein-protein in-plane interactions. The result is a high performance in foaming properties with nearly two times higher foam volumes and five times higher stability compared to GLOB-stabilised foams. The albumins present in FF and PM slightly increased the foamability compared to GLOB, but their foam stability is substantially lower than GLOB. Mild purification yields FF and PM with the highest protein nativity and presence of albumins, but these traits were not sufficient to boost their foaming performance. An underlaying reason could be the presence of more impurities in FF and PM. Further purification into GLOB increases the foam stability and yields the excellent foam stabiliser ALB as a side-stream.

Another promising ingredient are the protein coacervate colloids COL, which showed similar foamability, and even higher foam stability than ALB. We expect that the formed coacervate colloids with sizes between 400 and 2000 nm can block the lamellae or/and plateau borders between the air bubbles. As a result, the drainage and destabilisation processes were slowed down, leading to an extraordinarily high foam stability (>400 min). Simple coacervation is a relatively simple method to form protein colloids with good foaming properties. In addition, proteins in COL were able to form stiff interfacial films, which could be related to more hydrophobic interactions at the interface between the more hydrophobic COL. The exact interface and foam stabilising mechanism requires analysis in future studies.

In this work, we have shown the high potential of mung bean proteins as foam stabilisers. The ability to form and stabilise foam is intimately related to the fractionation used, as this affects the protein purity, protein composition, and presence of non-proteinaceous components. Exploring the different mild and sustainable protein fractionation routes to obtain protein ingredients with useful functional properties, can contribute to the creation of plant-based alternatives, thereby contributing to the current plant protein transition. Other protein sources and mung bean cultivars should also be studied using comparable fractionation methods to evaluate the transferability of our findings. Other functional properties should also receive attention, examples are emulsification, gelling and digestion.

## CRediT author statement

**Jack Yang**: Conceptualisation, Methodology, Investigation, Validation, Visualisation, Writing – Original Draft; **Qiuhuizi Yang**: Conceptualisation, Methodology, Investigation, Validation, Visualisation, Writing – Original Draft; **Babet Waterink**: Methodology, Investigation; Validation; **Paul Venema**: Conceptualisation, Methodology, Supervision, Writing – Review & Editing; **Renko de Vries**: Conceptualisation, Methodology, Supervision, Writing – Review & Editing; **Leonard M.C. Sagis**: Conceptualisation, Methodology, Supervision, Writing – Review & Editing.

## Declaration of competing interest

The authors have declared that no competing interest exist.

## Data availability

Data will be made available on request.

## Acknowledgements

The authors have declared that no competing interest exists. The authors thank Helene Mocking for her contribution in size exclusion chromatography. J. Yang acknowledges funding by TiFN, a public-private partnership on precompetitive research in food and nutrition. This research was performed with additional funding from the Netherlands Organisation for Scientific Research (NWO), and the Top Consortia for Knowledge and Innovation of the Dutch Ministry of Economic Affairs (TKI). NWO project number: ALWTF.2016.001. Q. Yang acknowledges financial support from China Scholarship Council (CSC).

## Appendix A. Supplementary data

Supplementary data to this article can be found online at https://doi.org/10.1016/j.foodhyd.2023.108885.

## References

Anwar, F., Latif, S., Przybylski, R., Sultana, B., & Ashraf, M. (2007). Chemical composition and antioxidant activity of seeds of different cultivars of mungbean. *Journal of Food Science, 72*(7), 503–510. https://doi.org/10.1111/j.1750-3841.2007.00462.x

Barać, M. B., Pešić, M. B., Stanojević, S. P., Kostić, A. Z., & Čabrilo, S. B. (2015). Techno-functional properties of pea (Pisum sativum) protein isolates-a review. *Acta Periodica Technologica, 46*, 1–18. https://doi.org/10.2298/APT1546001B

Bock, A., Steinhäuser, U., & Drusch, S. (2021). Partitioning behavior and interfacial activity of phenolic acid derivatives and their impact on β-lactoglobulin at the oil-water interface. *Food Biophysics, 16*, 191–202. https://doi.org/10.1007/s11483-020-09663-7

Brishti, F. H., Zarei, M., Muhammad, S. K. S., Ismail-Fitry, M. R., Shukri, R., & Saari, N. (2017). Evaluation of the functional properties of mung bean protein isolate for development of textured vegetable protein. *International Food Research Journal, 24*(4), 1595–1605.

Chen, M., Sala, G., Meinders, M. B. J., van Valenberg, H. J. F., van der Linden, E., & Sagis, L. M. C. (2017). Interfacial properties, thin film stability and foam stability of casein micelle dispersions. *Colloids and Surfaces B: Biointerfaces, 149*, 56–63. https://doi.org/10.1016/j.colsurfb.2016.10.010

Chéreau, D., Videcoq, P., Ruffieux, C., Pichon, L., Motte, J. C., Belaid, S., et al. (2016). Combination of existing and alternative technologies to promote oilseeds and pulses proteins in food applications. *OCL - Oilseeds and Fats, Crops and Lipids, 41*(1). https://doi.org/10.1051/ocl/2016020

Chua, J. Y., & Liu, S. Q. (2019). Soy whey: More than just wastewater from tofu and soy protein isolate industry. *Trends in Food Science and Technology, 91*, 24–32. https://doi.org/10.1016/j.tifs.2019.06.016

Denkov, N. D., & Marinova, K. G. (2006). Antifoam effects of solid particles, oil drops and oil–solid compounds in aqueous foams. In *Colloidal particles at liquid interfaces* (pp. 383–444). https://doi.org/10.1017/CBO9780511536670.011

Dhayal, S. K., Delahaije, R. J. B. M., de Vries, R. J., Gruppen, H., & Wierenga, P. A. (2015). Enzymatic cross-linking of α-lactalbumin to produce nanoparticles with increased foam stability. *Soft Matter, 11*(40), 7888–7898. https://doi.org/10.1039/C5SM01112D

Du, M., Xie, J., Gong, B., Xu, X., Tang, W., Li, X., et al. (2018). Extraction, physicochemical characteristics and functional properties of Mung bean protein. *Food Hydrocolloids, 76*, 131–140. https://doi.org/10.1016/j.foodhyd.2017.01.003

Ewoldt, R. H., Hosoi, A. E., & McKinley, G. H. (2007). New measures for characterizing nonlinear viscoelasticity in large amplitude oscillatory shear. *Journal of Rheology, 52*(6), 1427–1458. https://doi.org/10.1122/1.2970095

Ganesan, K., & Xu, B. (2018). A critical review on phytochemical profile and health promoting effects of mung bean (Vigna radiata). *Food Science and Human Wellness, 7*(1), 11–33. https://doi.org/10.1016/j.fshw.2017.11.002

Geerts, M. E. J., Nikiforidis, C.v., van der Goot, A. J., & van der Padt, A. (2017). Protein nativity explains emulsifying properties of aqueous extracted protein components from yellow pea. *Food Structure, 14*, 104–111. https://doi.org/10.1016/j.foostr.2017.09.001

Ghumman, A., Kaur, A., & Singh, N. (2016). Functionality and digestibility of albumins and globulins from lentil and horse gram and their effect on starch rheology. *Food Hydrocolloids, 61*, 843–850. https://doi.org/10.1016/j.foodhyd.2016.07.013

Gonzalez-Perez, S., & Vereijken, J. M. (2007). Sunflower proteins: Overview of their physicochemical, structural and functional properties. *Journal of the Science of Food and Agriculture, 87*, 2173–2191. https://doi.org/10.1002/jsfa

González-Pérez, S., Vereijken, J. M., van Koningsveld, G. A., Gruppen, H., & Voragen, A. G. J. (2005a). Formation and stability of foams made with sunflower (Helianthus annuus) proteins. *Journal of Agricultural and Food Chemistry, 53*(16), 6469–6476. https://doi.org/10.1021/jf0501793

Gonzalez-Perez, S., Vereijken, J. M., van Koningsveld, G. A., Gruppen, H., & Voragen, A. G. J. (2005b). Physicochemical Properties of 2S albumins and the corresponding protein isolate from Sunflower (Helianthus annuus). *Food Chemistry and Toxicology, 70*(1), C98–C103.

Hadidi, M., Jafarzadeh, S., & Ibarz, A. (2021). Modified mung bean protein: Optimization of microwave-assisted phosphorylation and its functional and structural characterizations. *LWT, 151*. https://doi.org/10.1016/j.lwt.2021.112119

Herneke, A., Karkehabadi, S., Lu, J., Lendel, C., & Langton, M. (2023). Protein nanofibrils from mung bean: The effect of pH on morphology and the ability to form and stabilise foams. *Food Hydrocolloids, 136*. https://doi.org/10.1016/j.foodhyd.2022.108315

He, Q., Zhang, Y., Lu, G., Miller, R., Möhwald, H., & Li, J. (2008). Dynamic adsorption and characterization of phospholipid and mixed phospholipid/protein layers at liquid/liquid interfaces. *Advances in Colloid and Interface Science, 140*(2), 67–76. https://doi.org/10.1016/j.cis.2007.12.004

Hinderink, E. B. A., Sagis, L., Schroën, K., & Berton-Carabin, C. C. (2020). Behavior of plant-dairy protein blends at air-water and oil-water interfaces. *Colloids and Surfaces B: Biointerfaces, 192*, Article 111015. https://doi.org/10.1016/j.colsurfb.2020.111015

Hoover, R., Li, Y. X., Hynes, G., & Senanayake, N. (1997). Physicochemical characterization of mung bean starch. *Food Hydrocolloids, 11*(4), 401–408. https://doi.org/10.1016/S0268-005X(97)80037-9

Inthavong, W., Chassenieux, C., & Nicolai, T. (2019). Viscosity of mixtures of protein aggregates with different sizes and morphologies. *Soft Matter, 15*(23), 4682–4688. https://doi.org/10.1039/c9sm00298g

Karaca, O. B., Güven, M., Yasar, K., Kaya, S., & Kahyaoglu, T. (2009). The functional, rheological and sensory characteristics of ice creams with various fat replacers. *International Journal of Dairy Technology, 62*(1), 93–99. https://doi.org/10.1111/j.1471-0307.2008.00456.x

Klafter, J., & Shlesinger, M. F. (1986). On the relationship among three theories of relaxation in disordered. *Proceedings of the National Academy of Sciences of the United States of America, 83*(4), 848–851. https://doi.org/10.1073/pnas.83.4.848

Kornet, C., Venema, P., Nijsse, J., van der Linden, E., van der Goot, A. J., & Meinders, M. (2020). Yellow pea aqueous fractionation increases the specific volume fraction and viscosity of its dispersions. *Food Hydrocolloids, 99*, Article 105332. https://doi.org/10.1016/j.foodhyd.2019.105332

Kornet, R., Yang, J., Venema, P., van der Linden, E., & Sagis, L. (2022). Optimizing pea protein fractionation to yield protein fractions with a high foaming and emulsifying capacity. *Food Hydrocolloids, 126*, Article 107456. https://doi.org/10.1016/j.foodhyd.2021.107456

Kudre, T. G., Benjakul, S., & Kishimura, H. (2013). Comparative study on chemical compositions and properties of protein isolates from mung bean, black bean and Bambara groundnut. *Journal of the Science of Food and Agriculture, 93*(10), 2429–2436. https://doi.org/10.1002/jsfa.6052

Lam, A. C. Y., Can Karaca, A., Tyler, R. T., & Nickerson, M. T. (2018). Pea protein isolates: Structure, extraction, and functionality. *Food Reviews International, 34*(2), 126–147. https://doi.org/10.1080/87559129.2016.1242135

Lie-Piang, A., Braconi, N., Boom, R. M., & van der Padt, A. (2021). Less refined ingredients have lower environmental impact – a life cycle assessment of protein-rich ingredients from oil- and starch-bearing crops. *Journal of Cleaner Production, 292*, Article 126046. https://doi.org/10.1016/j.jclepro.2021.126046

Liu, F. F., Li, Y. Q., Sun, G. J., Wang, C. Y., Liang, Y., Zhao, X. Z., et al. (2022). Influence of ultrasound treatment on the physicochemical and antioxidant properties of mung bean protein hydrolysate. *Ultrasonics Sonochemistry, 84*. https://doi.org/10.1016/j.ultsonch.2022.105964

Liu, H., Liu, H., Yan, L., Cheng, X., & Kang, Y. (2015). Functional properties of 8S globulin fractions from 15 mung bean (Vigna radiata (L.) Wilczek) cultivars. *International Journal of Food Science and Technology, 50*(5), 1206–1214. https://doi.org/10.1111/ijfs.12761

Loveday, S. M. (2020). Plant protein ingredients with food functionality potential. *Nutrition Bulletin, 45*(3), 321–327. https://doi.org/10.1111/nbu.12450

Lucassen, J., & van den Tempel, M. (1972). Dynamic measurements of dilational properties of a liquid interface. *Chemical Engineering Science, 27*(6), 1283–1291. https://doi.org/10.1016/0009-2509(72)80104-0

Lu, B. Y., Quillien, L., & Popineau, Y. (2000). Foaming and emulsifying properties of pea albumin fractions and partial characterisation of surface-active components. *Journal of the Science of Food and Agriculture, 80*(13), 1964–1972. https://doi.org/10.1002/1097-0010(200010)80:13<1964::AID-JSFA737>3.0.CO;2-J

Mariotti, F., Tomé, D., & Mirand, P. P. (2008). Converting nitrogen into protein - beyond 6.25 and Jones' factors. *Critical Reviews in Food Science and Nutrition, 48*(2), 177–184. https://doi.org/10.1080/10408390701279749

Mendoza, E. M. T., Adachi, M., Bernardo, A. E. N., & Utsumi, S. (2001). Mungbean [Vigna radiata (L.) Wilczek] globulins: Purification and characterization. *Journal of Agricultural and Food Chemistry, 49*(3), 1552–1558. https://doi.org/10.1021/jf001041h

Möller, A. C., van der Padt, A., & van der Goot, A. J. (2021). From raw material to mildly refined ingredient – linking structure to composition to understand fractionation processes. *Journal of Food Engineering, 291*. https://doi.org/10.1016/j.jfoodeng.2020.110321

Mubarak, A. E. (2005). Nutritional composition and antinutritional factors of mung bean seeds (Phaseolus aureus) as affected by some home traditional processes. *Food Chemistry, 89*(4), 489–495. https://doi.org/10.1016/j.foodchem.2004.01.007

Ntone, E., Wesel, T. Van, Sagis, L. M. C., Meinders, M., Bitter, J. H., & Nikiforidis, C. V. (2021). Adsorption of rapeseed proteins at oil/water interfaces . Janus-like napins dominate the interface. *Journal of Colloid and Interface Science, 583*, 459–469. https://doi.org/10.1016/j.jcis.2020.09.039

Osborne, T. B. (1924). *The vegetable proteins*. Longmans green and co.

Pelgrom, P. J. M., Boom, R. M., & Schutyser, M. A. I. (2014). Functional analysis of mildly refined fractions from yellow pea. *Food Hydrocolloids, 44*, 12–22. https://doi.org/10.1016/j.foodhyd.2014.09.001

Pernollet, J. C. (1978). Protein bodies of seeds: Ultrastructure, biochemistry, biosynthesis and degradation. *Phytochemistry, 17*(9), 1473–1480. https://doi.org/10.1016/S0031-9422(00)94623-5

Rühs, P. A., Affolter, C., Windhab, E. J., & Fischer, P. (2013). Shear and dilatational linear and nonlinear subphase controlled interfacial rheology of β-lactoglobulin fibrils and their derivatives. *Journal of Rheology, 57*(3), 1003–1022. https://doi.org/10.1122/1.4802051

Rullier, B., Axelos, M. a V., Langevin, D., & Novales, B. (2009). β-Lactoglobulin aggregates in foam films: Correlation between foam films and foaming properties. *Journal of Colloid and Interface Science, 336*(2), 750–755. https://doi.org/10.1016/j.jcis.2009.04.034

Rullier, B., Novales, B., & Axelos, M. A. V. (2008). Effect of protein aggregates on foaming properties of β-lactoglobulin. *Colloids and Surfaces A: Physicochemical and Engineering Aspects, 330*(2–3), 96–102. https://doi.org/10.1016/j.colsurfa.2008.07.040

Sagis, L. M. C., Liu, B., Li, Y., Essers, J., Yang, J., Moghimikheirabadi, A., et al. (2019). Dynamic heterogeneity in complex interfaces of soft interface-dominated materials. *Scientific Reports, 9*(1), 1–12. https://doi.org/10.1038/s41598-019-39761-7

Sağlam, D., Venema, P., De Vries, R., & Van Der Linden, E. (2013). The influence of pH and ionic strength on the swelling of dense protein particles. *Soft Matter, 9*(18), 4598–4606. https://doi.org/10.1039/c3sm50170a

Sandoval-Castilla, O., Lobato-Calleros, C., Aguirre-Mandujano, E., & Vernon-Carter, E. J. (2004). Microstructure and texture of yogurt as influenced by fat replacers. *International Dairy Journal, 14*(2), 151–159. https://doi.org/10.1016/S0958-6946(03)00166-3

Shewan, H. M., & Stokes, J. R. (2013). Review of techniques to manufacture micro-hydrogel particles for the food industry and their applications. *Journal of Food Engineering, 119*(4), 781–792. https://doi.org/10.1016/j.jfoodeng.2013.06.046

Shrestha, S., van 't Hag, L., Haritos, V. S., & Dhital, S. (2023). Lentil and Mungbean protein isolates: Processing, functional properties, and potential food applications. In *Food hydrocolloids* (Vol. 135). Elsevier B.V. https://doi.org/10.1016/j.foodhyd.2022.108142

Souza, P. F. N. (2020). The forgotten 2S albumin proteins: Importance, structure, and biotechnological application in agriculture and human health. *International Journal of Biological Macromolecules, 164*, 4638–4649. https://doi.org/10.1016/j.ijbiomac.2020.09.049

Tamayo Tenorio, A., Kyriakopoulou, K. E., Suarez-Garcia, E., van den Berg, C., & van der Goot, A. J. (2018). Understanding differences in protein fractionation from conventional crops, and herbaceous and aquatic biomass - consequences for industrial use. *Trends in Food Science and Technology, 71*(November 2017), 235–245. https://doi.org/10.1016/j.tifs.2017.11.010

Tang, C. H., & Sun, X. (2010). Physicochemical and structural properties of 8S and/or 11S globulins from mungbean [Vigna radiata (L.) Wilczek] with various polypeptide constituents. *Journal of Agricultural and Food Chemistry, 58*(10), 6395–6402. https://doi.org/10.1021/jf904254f

Watts, C., & Davies, E. (1969). Non-symmetrical dielectric relaxation behaviour arising from a simple empirical decay function. *Transactions of the Faraday Society, 66*(1), 80–85. https://doi.org/10.1039/TF9706600080

Xia, W., Botma, T., Sagis, L. M. C., & Yang, J. (2022). Selective proteolysis of β-conglycinin as a tool to increase air-water interface and foam stabilising properties of soy proteins. *Food Hydrocolloids, 130*, Article 107726. https://doi.org/10.1016/j.foodhyd.2022.107726

Yang, J., de Wit, A., Diedericks, C. F., Venema, P., van der Linden, E., & Sagis, L. M. C. (2022). Foaming and emulsifying properties of extensively and mildly extracted Bambara groundnut proteins: A comparison of legumin, vicilin and albumin protein. *Food Hydrocolloids, 123*, Article 107190. https://doi.org/10.1016/j.foodhyd.2021.107190

Yang, J., Kornet, R., Diedericks, C. F., Yang, Q., Berton-Carabin, C. C., Nikiforidis, C.v., et al. (2022). Rethinking plant protein extraction: Albumin — from side stream to an excellent foaming ingredient. *Food Structure, 31*, Article 100254. https://doi.org/10.1016/j.foostr.2022.100254

Yang, J., Thielen, I., Berton-Carabin, C. C., van der Linden, E., & Sagis, L. M. C. (2020). Nonlinear interfacial rheology and atomic force microscopy of air-water interfaces stabilized by whey protein beads and their constituents. *Food Hydrocolloids, 101*, Article 105466. https://doi.org/10.1016/j.foodhyd.2019.105466

Yang, Q., Venema, P., van der Linden, E., & de Vries, R. (2023). Soluble protein particles produced directly from mung bean flour by simple coacervation. *Food Hydrocolloids, 139*. https://doi.org/10.1016/j.foodhyd.2023.108541

Yang, J., Waardenburg, L. C., Berton-Carabin, C. C., Nikiforidis, C.v., van der Linden, E., & Sagis, L. M. C. (2021). Air-water interfacial behaviour of whey protein and rapeseed oleosome mixtures. *Journal of Colloid and Interface Science, 602*, 207–221. https://doi.org/10.1016/j.jcis.2021.05.172

Yi-Shen, Z., Shuai, S., & Fitzgerald, R. (2018). Mung bean proteins and peptides: Nutritional, functional and bioactive properties. *Food & Nutrition Research, 62*, 1–11. https://doi.org/10.29219/fnr.v62.1290

Zhang, Y., Chang, Z., Luo, W., Gu, S., Li, W., & An, J. (2015). Effect of starch particles on foam stability and dilational viscoelasticity of aqueous-foam. *Chinese Journal of Chemical Engineering, 23*(1), 276–280. https://doi.org/10.1016/j.cjche.2014.10.015